2025 IEEE World Haptics Conference (WHC)
Suwon Convention Center, Suwon, Korea
July 8 ~ 11, 2025

Force is all you need? Rethinking Acoustic-Only Prediction of Mid-Air Haptics Perceived Strength

Noor Alakhawand
Ultraleap Ltd
Bristol, UK
0000-0003-1435-1808

Dario Pittera
Ultraleap Ltd
Bristol, UK
0000-0001-7537-0266

Stefano Tronci
Ultraleap Ltd
Bristol, UK

Orestis Georgiou
Ultraleap Ltd
Bristol, UK
0000-0003-2303-6754

William Frier
Ultraleap Ltd
Bristol, UK
0000-0002-0311-720X

***Abstract*—Mid-air haptic systems use focused ultrasound to create tactile sensations in free space. However, predicting and calibrating these systems according to human perception often requires complex multi-physics models or lengthy user studies. In this work, we address this challenge by conducting an extensive measurement campaign, capturing perceived intensity, acoustic pressure, and force across varying heights and device voltages. Using this data, we evaluate four linear models to predict perceived intensity, culminating in a model that combines normalized force and distance. This model achieves strong predictive accuracy, demonstrating that force is a practical and effective predictor of perceived intensity. Our findings show that force, measured using an affordable precision scale, offers a straightforward alternative to complex pressure-based approaches, providing an accessible framework for characterizing mid-air haptic systems. This approach enables efficient, perception-driven design and optimization of mid-air haptic applications.**

***Index Terms*—mid-air haptics, ultrasound, perception, model.**

I. Introduction

Mid-air haptic systems use ultrasound arrays comprising hundreds of transducers to electronically focus and modulate acoustic waves which impinge the users' skin, thus creating vibrotactile contactless sensations [1], [2]. Enabled by this discovery, the haptic and human-computer-interaction (HCI) research communities have over the past decade explored and characterized numerous applications and capabilities of the technology. For example, these systems have found applications in virtual and augmented reality (VR/AR) for displaying tactile holographic objects [3]–[6], automotive user interfaces for displaying touchless controls and mid-air notifications [7]–[9], as well as in medical training simulations to emulate the palpation of a virtual patient [10], [11].

An inherent limitation of mid-air haptics has always been that the perceived tactile stimulus intensity was rather weak, as compared to other contact-based haptic interfaces like force-feedback, wearables, or surface-haptics. To that end, major efforts have been aimed at addressing this limitation following predominantly one of two possible approaches: (i) hardware size/shape, (ii) signal modulation. The former approach (i) aims to drive more power to the focused ultrasound tactile stimulus using more or better-positioned transducer arrays. Tackling the electronic and hardware complexities has been recently reviewed by Inoue et al. [12], however a plethora of physical phenomena such as acoustic attenuation, absorption, and saturation impose physical limits on how much acoustic pressure can be concentrated in a mid-air ultrasonic focus [13], [14]. The latter approach, (ii) aims to maximize the perceived intensity or alter the emotional tone of the tactile stimulus by means of waveform signal processing, and has been recently reviewed by Hasegawa et al. [15]. Basically, different waveforms and spatiotemporal modulations can create different indentation patterns on the user's skin [16], [17] which in effect can influence the user's perceptual (intensity/texture) and emotional (valence/arousal) responses [18] [19].

Regardless of the approach taken, understanding how the perceived intensity varies with device and stimulus parameters is essential for optimizing user experience, ensuring consistent system calibration, and improving energy efficiency, as argued by numerous authors [20]–[22]. This task however is made extra difficult by the large variety of mid-air haptic devices currently available, the lack of consistent and comprehensive data, and the complexity of simulation and predictive models.

To that end, in this paper we address these three identified difficulties by: (1) characterizing a 16×16 mid-air haptic display which is currently the most commonly used mid-air haptics device, (2) publishing a comprehensive measurement dataset (see Tables I - III), and (3) providing a simple yet effective model for predicting perceived intensity using force measurements (see equation (1)).

II. Related Works

Previous research has explored the relationship between acoustic pressure and tactile perception, but these studies often neglect the role of force or rely on idealized models that overlook non-linear effects. Studies in haptic perception have also investigated subjective responses but lack integration with physical measurements. Our work bridges these gaps by combining physical and perceptual data.

A. Force as a Predictor in Mid-Air Haptics

Force has been a key invariant in predicting perceived tactile intensity in prior mid-air haptics studies. Raza et al. [20] proposed a systematic mapping of device parameters to user perception by accounting for force, showing its strong

This work was supported by UKRI Future Leaders Fellowship (MR/W013576/1) and by EU Horizon 2020 (101017746).

correlation with perceptual feedback across various input configurations. Similarly, Fan et al. [21] integrated force feedback with ultrasonic haptic devices to create synergistic haptic effects, emphasizing the value of force in enhancing perceptual realism. Moreover, Morisaki et al. [23], [24] studied how lateral and amplitude modulation techniques can manipulate output forces, demonstrating the perceptual effects of subtle, non-vibratory static forces, which highlight force as a critical component in mid-air haptic rendering.

B. Acoustic Pressure as a Perceptual Metric

Acoustic pressure has also been extensively studied as a driver of perception models. Shen et al. [22] developed a two-stage predictive model for multi-point spatiotemporal modulation, linking acoustic pressure and other physical parameters to perceived tactile intensity. Morisaki et al. [25] compared acoustic measurements and perceptual reports of different modulation techniques, while Inoue et al. [3] and Mulot et al. [26] studied how the acoustic pressure distribution fields of mid-air haptic effects influence perception. All these works, and many others, tend to bypass force considerations, focusing solely on the acoustic field and modulation characteristics.

C. Gaps in Comparative Analyses

While both force and acoustic pressure have been independently studied as predictors of tactile perception, a direct comparison of their predictive strengths remains unexplored. Furthermore, most literature is focused on fixed spatial configurations, neglecting how perceptual outcomes vary with distance from the haptic device source. This gap is particularly significant since both acoustic pressure and force diminish with distance due to energy dispersion and system losses.

This paper builds on the existing literature by addressing these gaps. Namely, we systematically compare acoustic pressure and haptic force as predictors of perceived tactile intensity, integrating these metrics into a unified framework. By conducting perceptual, acoustic, and force experiments at varying distances (5 cm to 30 cm) and voltages (20, 24, and 28 V) as to alter the output acoustic pressures, we provide new insights into how spatial and device power parameters influence perception. To our knowledge, this is the first work to empirically map these relationships and propose a simple yet accurate model for capturing the interplay between pressure P, force F, height z, and perceived intensity I.

III. Methods

A. Study 1: Perceived Intensity Measurements

This perceptual study seeks to provide psychophysical insight into mid-air haptic perceived intensity, setting the foundation for our perceptual modelling.

1) Participants: We tested a total of 12 participants (11 males, age $\mu = 35.75$, SD $\pm$ 4.06, palm width $\mu = 66.25$, SD $= 7.94$). The palm width was measured on the upper palm from the index finger bone to the little finger bone. They had normal or glasses/lens-corrected vision and no history of neurological or psychological disorders. All participants were right-handed. Participants signed a consent form prior to taking part in the study which was reviewed and approved by an ethics committee.

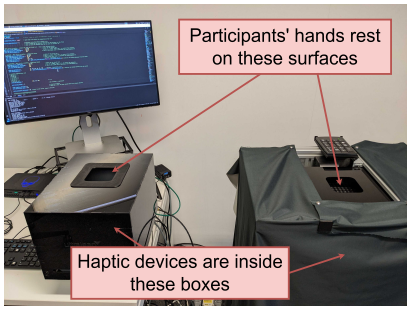

Fig. 1. Perception study setup: participants rested their palms on the two haptic devices located in the boxes. On the left, the haptic device used as a modulus. On the right, the device rendering the comparison stimulus, mounted on a linear actuator to vary the distance z between device and palm. Participants could enter their answers through a numeric pad.

2) Psychophysical Procedure and Stimuli: We employed a Magnitude Estimation Task with a Two-alternative Forced Choice procedure. Specifically, we rendered two mid-air haptic sensations at the same time from two ultrasound devices (both consisting of $16 \times 16 = 256$ transducers); one was outputting a fixed sensation used as an anchor point (modulus) with a fixed arbitrary value of 100. The other one rendered the comparison stimuli: a 2 cm radius circle sensation at full intensity presented at six different heights, which is the distance between the stimulus and the participants' hands, (z =5, 10, 15, 20, 25, and 30 cm) and at three different voltages (20, 24, and 28 V) giving a total of 18 stimuli. The modulus stimulus was also a 2 cm radius circle sensation fixed at z =10 cm height at 80% output intensity from a haptic device driven at 20 V. Each comparison stimulus was repeated five times at each height to minimize the variance of the participant answers. Thus, each participant was exposed to 90 stimuli. Further, as it was not possible to change the input voltage in useful time for the experiment, we counterbalanced the orders of voltage appearance in blocks, i.e., one participant started with voltage sequence 20, 24, 28, the next with 28, 20, 24, and so on.

The participants would feel the stimulus for one second on the center of their palm. At the start of the experiment, a focal point was emitted so that participants could adjust their hand to the desired location. The participants rated the intensity of the test stimulus by comparing it to the modulus using a keyboard and a GUI as seen in Figure 1. For instance, if they felt the comparison stimulus was twice as strong, they would enter 200, if half as strong, 50, if the same, 100, and so on.

3) Experimental Apparatus: Two haptic devices were used, each consisting of 256 ultrasound transducers, positioned inside two laser-cut acrylic boxes with a 9.5×9.5 cm aperture. The device used as the modulus was located 10 cm below the box aperture. The device used to deliver the comparison stimuli was mounted on a linear actuator to allow varying its distance z from the participants' palm (see Figure 1). The comparison device would automatically adjust the ultrasound

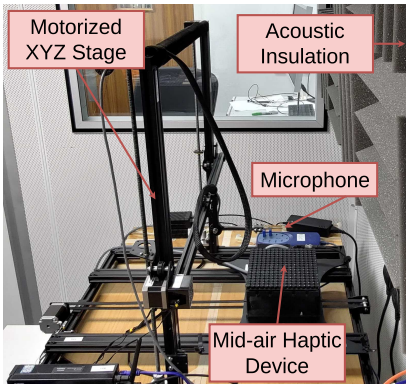

Fig. 2. Details of the pressure measurement setup.

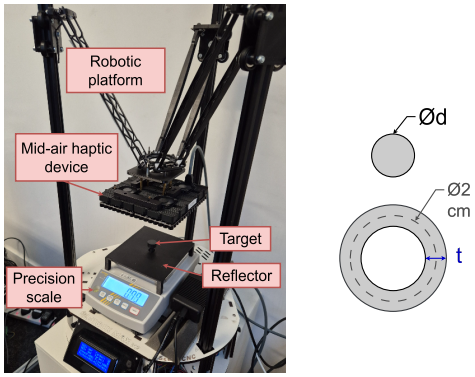

(a) Force measurement setup (b) Targets

Fig. 3. (a) Details of the force measurement setup. (b) Target shapes for force measurement.

focusing stimulus according to the device-to-hand distance z.

B. Study 2: Acoustic Pressure Measurements

1) Objective: To measure the acoustic pressure produced by mid-air haptic devices when rendering the stimuli described in Study 1, as a function of height z and input voltages.

2) Setup: Placing the mid-air haptic device inside an acoustically treated room and using a motorized XYZ stage, a calibrated microphone (B&K Type 4138-A-015) was used to record the pressure time-series across a predefined spatial grid at a reference height of 10 cm (see Figure 2). The pressure time series were processed to obtain an overall root mean square (RMS) value. This allowed us to find the xy location of maximal RMS in the field. Then, the acoustic pressure time-series was recorded at this xy location, but at heights ranging from z =5 cm to 30 cm at 5 cm increments from the device, under varying input voltage conditions, 20, 24, and 28 V. In each case, the haptic device would automatically re-adjust the ultrasonic focusing according to z so that the microphone was always at the location of maximal RMS pressure. Note that microphones have a frequency response and a directivity, meaning that microphone orientation matters. For this study we rendered near axis sensations, meaning that the wavefront direction was near vertical. Therefore, we opted for horizontal microphone orientation. This because at 90 degree incidence the frequency response is flat, which helps preventing capsule and/or preamp non-linearity. This allows reproducible and repeatable results for all measurements. Also note, that the transducers of the mid-air haptics system were driven by a PWM signal. Due to the transducers being highly resonant devices, the higher harmonics of the PWM can be neglected. In this study, the input voltage being varied was the peak-to-peak voltage of the PWM, while its duty was kept to 50%.

3) Post-Processing: The pressure time series were recorded for a duration of 1 s. To limit the error due to noise and distortion products at the microphone level, the time series were filtered by a pass-band filter centred on the carrier frequency. The overall RMS value was computed from the whole filtered time series.

C. Study 3: Force Measurements

1) Objective: To quantify the force produced by the haptic device at varying heights and input voltages.

2) Setup: A precision scale (Kern-PCB 2500-2) with an accuracy of 0.01 g was used to measure the force. A target acrylic pillar was placed on the precision scale, of varying shapes and sizes (see Figure 3) as to match ultrasonic stimulus:

- Circle: force was measured for unmodulated (UM) device output focused onto the cylindrical pillars with diameters d of 1 cm, 2 cm, and 3 cm.
- Annulus: force was measured for Spatiotemporally Modulated (STM) device output focused onto a hollow cylindrical pillar (i.e., an annulus) with inner diameter of 2 cm (to match the diameter of the rendered STM circle stimulus) with thickness t of 1 cm, 2 cm, and 3 cm.

A reflector plate was placed around and inside the pillars to shield the precision scale from the acoustic field that does not hit the pillar. The haptic device was positioned above the precision scale, held by a robotic platform that could move the haptic device up and down as needed.

3) Post-Processing: The force data was collected from the precision scale as time series data over 10 seconds. The precision scale takes 3 seconds to stabilize its measurement, and the force can slightly fluctuate over time. We take the mean of the time series data at the steady state as the true force measurement. This process is repeated three times for each parameter set to reduce noise, and the average was reported.

IV. Results

In this section, we report and briefly discuss the data collected from the measurement campaign reported in the previous section. All data is also reported in Tables I-III.

A. Study 1: Perceived Intensity Findings

Figure 4 illustrates how the perceived intensity varies with changes in input voltage and the height (distance between the hand and the focal point). Notably, a quadratic trend emerges: perception is minimal at smaller heights ($\sim$5 cm) and larger heights ($\sim$ >20 cm). The perceived intensity peaks between

TABLE I
EXPERIMENTAL DATA 20 VOLTS

z (cm)	Perceived Intensity	Force (g) UM 1cm	Force (g) UM 2cm	Force (g) UM 3cm	Force (g) STM 1cm	Force (g) STM 2cm	Force (g) STM 3cm	Acoustic STM RMS (Pa)
5	88.27	0.44	0.50	0.57	0.48	0.58	0.65	923.97
10	106.33	0.73	0.91	0.99	0.74	0.89	0.94	935.39
15	112.08	0.82	1.06	1.15	0.95	1.16	1.20	854.28
20	104.50	0.89	1.13	1.18	0.97	1.24	1.31	759.50
25	100.23	0.79	1.09	1.16	0.90	1.25	1.30	682.69
30	90.42	0.59	0.90	1.06	0.79	1.19	1.29	596.08

TABLE II
EXPERIMENTAL DATA 24 VOLTS

z (cm)	Perceived Intensity	Force (g) UM 1cm	Force (g) UM 2cm	Force (g) UM 3cm	Force (g) STM 1cm	Force (g) STM 2cm	Force (g) STM 3cm	Acoustic STM RMS (Pa)
5	90.50	0.50	0.65	0.75	0.60	0.75	0.81	1022.55
10	112.08	0.90	1.13	1.27	0.94	1.13	1.17	1032.67
15	116.08	0.95	1.31	1.43	1.18	1.45	1.51	962.77
20	111.25	1.05	1.35	1.50	1.16	1.53	1.59	813.02
25	104.72	0.95	1.24	1.38	1.06	1.49	1.61	712.02
30	92.50	0.70	0.99	1.13	0.93	1.36	1.57	616.66

TABLE III
EXPERIMENTAL DATA 28 VOLTS

z (cm)	Perceived Intensity	Force (g) UM 1cm	Force (g) UM 2cm	Force (g) UM 3cm	Force (g) STM 1cm	Force (g) STM 2cm	Force (g) STM 3cm	Acoustic STM RMS (Pa)
5	105.00	0.63	0.81	0.91	0.71	0.88	1.00	1107.14
10	129.75	1.09	1.35	1.48	1.12	1.35	1.43	1122.95
15	128.58	1.11	1.56	1.66	1.39	1.71	1.80	1019.73
20	118.37	1.19	1.59	1.73	1.34	1.76	1.88	863.27
25	109.42	0.98	1.44	1.57	1.25	1.72	1.89	741.53
30	95.75	0.64	1.18	1.30	1.08	1.58	1.79	646.26

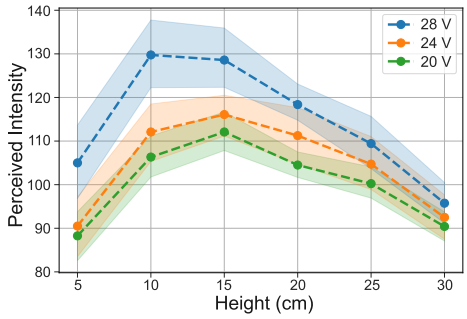

Fig. 4. Perceived intensity plots as a function of the height focusing distance.

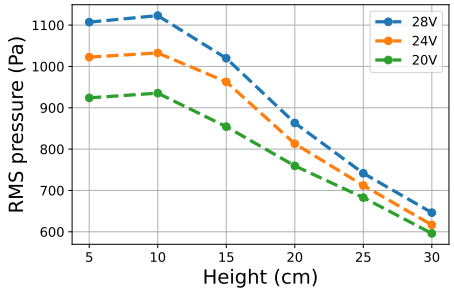

Fig. 5. Acoustic pressure measurements in Pascals as a function of the height focusing distance z.

10 cm and 15 cm. As expected, higher voltages correspond to greater perceived intensity.

B. Study 2: Acoustic Pressure Findings

Figure 5 shows the RMS pressure for the voltages tested, as a function of height. It is possible to see that overall the pressure decreases with distance. This has to be expected, as sound naturally decays moving away from a source.

All curves have a maximum at 10 cm of height. This is due to the combined effects of transducer directivity and array layout. At 10 cm the driving voltage clearly affects the pressure, the gap between the curves amounting to $\sim$100 Pa. However, the effect of voltage is not as significant for larger heights. This is likely due to the combined effects of in-air absorption and acoustic saturation.

This data illustrates that the pressure field is directly influenced by both the driving voltage applied to the transducers and the distance from the haptic device. It is therefore natural to expect perception to be influenced by factors directly connected to height and acoustic quantities related to pressure.

C. Study 3: Force Findings

The measurements presented in Figure 6 show that force does not follow the same trend as the acoustic pressure measurements. This is because the measured force produced by the

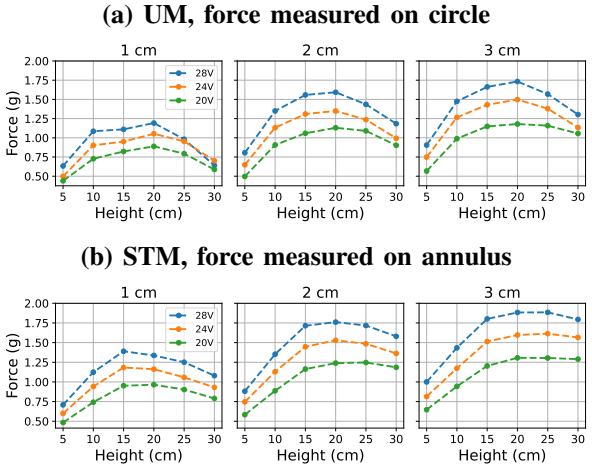

Fig. 6. Force measurements on targets with different sizes for varying heights and voltages. (a) The force is measured for unmodulated (UM) haptic device output on circles with diameters 1 cm, 2 cm, and 3 cm. (b) The force is measured for spatiotemporal modulation (STM) haptic device output on annulus with thicknesses of 1 cm, 2 cm, and 3 cm.

device is not only dependent on the RMS acoustic pressure at the focus but also on the wave direction and pressure distribution. We know that the height of the focus changes the pressure distribution, with larger heights producing larger focal points with width $w = 2\lambda z/A$, where λ is the wavelength and A the device aperture [27]. Thus, if the acoustic pressure at the focus remains constant but the focal point's width w changes with height z, then the force measured (an integral of pressure over the acrylic pillar's surface area) at lower heights will be less than that at higher heights. Also, at lower focusing heights, waves coming from the perimeter of the device will have a smaller force component that is perpendicular to the force balance surface. This explains the left half of the parabolas observed in Figure 6. The right half of the force parabolas is due to the drop in pressure at larger heights.

Figure 6(a) shows the measurements of force output for an unmodulated (UM) haptic device output on circular targets with diameters 1 cm, 2 cm, and 3 cm. The results show that the force initially increases with height until it reaches a peak at 20 cm, and then decreases with height after that. As expected, larger target sizes lead to larger forces measured, as more of the acoustic field is captured in the measurement.

Figure 6(b) shows the measurements of force for the spatiotemporally modulated (STM) stimulus output measured on the annulus-shaped targets with varying thicknesses of 1 cm, 2 cm, and 3 cm. The results again show that the force initially increases with height until it reaches a peak at around 15 or 20 cm and then decreases with height after that. Additionally, larger target sizes lead to larger forces measured. Increasing the voltage leads to an increase in force.

Next, the date was used to calculate the Pearson correlation coefficient ρ (which measures the linear correlation between two variables) for the force measurements against the perceived intensity to see which measurement type (UM vs. STM, 1 cm vs. 2 cm vs. 3 cm) is the most highly correlated with perceived intensity (Table IV). The calculations show that the UM force measurement on the 1 cm circle has the highest correlation coefficient with perceived intensity ($\rho = 0.87$). Therefore, we choose this force measurement type going forward.

TABLE IV
PEARSON CORRELATION COEFFICIENT FOR FORCE VS. INTENSITY

Measurement type	1 cm	2 cm	3 cm
UM, circle target	0.87	0.78	0.76
STM, annulus target	0.74	0.54	0.47

V. MODEL FITTING

To investigate the relationship between perceived intensity I and the measured physical quantities, we proposed a set of four linear models. These models use the measured RMS acoustic pressure P (in Pascals), measured force on a 1 cm target F (in gram force), and distance from the device z (in meters) to predict the perceived intensity I, which is a unitless quantity relative to the comparison modulus stimulus (a 2 cm radius STM circle sensation fixed at $z = 0.10$ m).

The following four simple linear models are tested:

1) $I(P) = c_0 + c_1 \frac{P}{P_0}$
2) $I(F) = c_0 + c_1 \frac{F}{F_0}$
3) $I(P, z) = c_0 + c_1 \frac{P}{P_0} + c_2 \frac{z}{z_0}$
4) $I(F, z) = c_0 + c_1 \frac{F}{F_0} + c_2 \frac{z}{z_0}$

Here, c_0, c_1, c_2 are the fitting coefficients to be determined for each model, and the variables are normalized by the modulus stimulus which was measured to output as follows:

- $P_0 = 742\,\text{Pa}$ is the reference pressure.
- $F_0 = 0.51\,\text{g-force}$ is the reference force output.
- $z_0 = 10\,\text{cm} = 0.1\,\text{m}$ is the reference distance.

This normalization ensures that all input variables are dimensionless and that the fitting coefficients represent the relative contributions of these normalized variables. Also, this procedure ensures that our model is independent of the Voltage used in the test stimulus.

The coefficients c_0, c_1, c_2 are determined using a least-squares regression for each model. The models are fitted to the dataset of perceived intensity measurements and corresponding values of P, F, and z. For each fit, the following metrics are computed:

- The coefficient of determination (R^2) to assess the goodness of fit.
- The root mean square error (RMSE) to evaluate the model's predictive accuracy.
- The mean absolute percentage error (MAPE) quantifies the average relative error as a percentage of observed values, providing an intuitive measure of model accuracy.

In the interest of simplicity, more advanced models with higher-order and cross-terms were not considered, even though they would probably further improve fitting accuracy at the expense of increased complexity (i.e., more coefficients $c_{i\geq 3}$), hence, harder interpretability. Next, the performance of our

four models will be compared based on these metrics to determine which variables (P, F, and/or z) provide the best predictive capability for I.

VI. Model Results and Discussion

The results of the regression analysis, including the fitted coefficients and performance metrics, are reported in Table V. These results demonstrate that, without accounting for height z, a model based only on force $I(F)$ outperforms one based only on pressure $I(P)$, as evidenced by the higher R^2 value and lower RMSE and MAPE for the force-based model.

TABLE V
Fitted Coefficients, R^2, RMSE, and MAPE for Each Model

Model	c_0	c_1	c_2	R^2	**RMSE**	**MAPE**
1. $I(P)$	74.04	28.09	–	0.27	10.15	7.6%
2. $I(F)$	65.61	25.05	–	0.76	5.69	4.7%
3. $I(P, z)$	-60.82	109.83	23.19	0.72	6.26	5.1%
4. $I(F, z)$	71.60	26.67	-4.93	0.88	3.98	3.3%

However, when including height z in the fitted model, the best-performing model is Model 4, $I(F, z) = c_0 + c_1 \frac{F}{F_0} + c_2 \frac{z}{z_0}$. It achieves the highest R^2 value (0.88) and the lowest RMSE (3.98) and MAPE (3.3%). Model 4, $I(F, z)$ provides the most accurate predictions of perceived intensity I, accounting for both the normalized force (F/F_0) and distance (z/z_0). Moreover, the inclusion of the distance parameter z improved the model's explanatory power compared to simpler linear models, reflecting how spatial variations in the ultrasound field significantly influence mid-air haptic perception.

This conclusion is particularly relevant given the practical limitations and high cost of measuring acoustic pressure. The few types of microphones capable of measuring ultrasound at these intensities are typically expensive and require additional specialized equipment, such as signal conditioners, high-speed analog-to-digital converters, and acoustic treatment of test chambers. Furthermore, their usage is made more challenging by issues of microphone directivity, limited bandwidth, and internal nonlinearity, all of which can affect the accuracy and consistency of pressure measurements.

In contrast, a standard precision scale offers an affordable and straightforward alternative for measuring the force output. It simplifies the experimental setup while maintaining predictive power over perceived intensity, as demonstrated by the strong performance of both force-based Models 2, $I(F)$, and 4, $I(F, z)$. The utility of force measurements is further underscored by their physical ability to provide a single, spatio-temporally integrated metric that captures the cumulative effects of the acoustic field, surpassing the limitations and complexities of microphone pressure measurements.

Importantly, to predict the perceived intensity of new haptic stimuli relative to modulus stimuli, practitioners and researchers alike can now leverage our proposed Model 4, $I(F, z)$, by obtaining a single force measurement F at the desired distance z. Specifically, given any known reference values (F_0, P_0, z_0), either from the Tables I-III we have provided, or from measurements outputted by a 16×16 transducer device, the normalized force (F/F_0) and distance (z/z_0) can be computed and substituted into the fitted equation:

$$I(F, z; F_0, z_0) = 71.60 + 26.67 \frac{F}{F_0} - 4.93 \frac{z}{z_0}. \quad (1)$$

This approach is practical and efficient because it eliminates the need for complex acoustic pressure measurements (P) and directly relates the readily measurable force to the perceived intensity. For example, suppose we want to estimate the relative perceived intensity of the stimulus with the highest measured force ($F = 1.19\,\text{g-force}$) at 28 volts, and at a distance of $z = 0.20\,\text{m}$, compared to the reference stimulus with the lowest measured force ($F_0 = 0.44\,\text{g-force}$) at 20 volts, and at $z_0 = 0.05\,\text{m}$. These values were taken from the Force UM 1 cm column in Tables I and III. Substituting these into equation (1) we calculate that the relative perceived intensity is approximately $I \approx 124.16 \pm 3.72$, where the relative error was obtained via the 3.3% MAPE of our model, indicating that the higher-force stimulus would be perceived as about 24.16% stronger than the lower-force reference.

Thus, by relying on a single force measurement and the distance from the device, this useful model allows for rapid and accurate predictions of perceived intensity in real-world applications, such as calibrating haptic feedback for VR/AR systems or designing new mid-air haptic automotive interfaces.

Limitations: The models presented in the paper are limited to mid-air haptic devices which are of similar size and shape to the haptic device used, within the 5–30 cm range, using 2 cm circle sensations which are centered around the *xy*-axis, and force measurements on a 1 cm target pillar. These constraints reflect the experimental setup. Extending the model to other configurations (e.g. new hardware or stimulus) would require additional validation. Finally, future studies should prioritize demographic variations (e.g. age, sex, or handness) to ensure that conclusions can be drawn from a broader population.

VII. Conclusion

This work was motivated by the need to predict and calibrate mid-air haptic systems according to human perception while avoiding the complexity of non-linear acoustic [14] and multi-physics models [16], as well as lengthy user studies [20], [22]. To address this, we conducted an extensive measurement campaign, capturing data for perceived intensity, acoustic pressure, and force across varying heights and device voltages. We then evaluated four linear models, each aimed at predicting perceived intensity using combinations of these physical parameters. The best-performing model, $I(F, z) = c_0 + c_1 \frac{F}{F_0} + c_2 \frac{z}{z_0}$, achieved strong predictive accuracy with an R^2 of 0.88, RMSE of 3.98, and MAPE of 3.3%. This model demonstrates that force, combined with distance, is a practical and effective predictor of perceived intensity.

Our findings provide a framework for calibrating mid-air haptic systems using simple force measurements, eliminating the need for expensive and complex pressure sensors or multi-physics simulations. Future work could expand this approach by extending the analysis to more diverse haptic scenarios.

REFERENCES

[1] T. Hoshi, M. Takahashi, T. Iwamoto, and H. Shinoda, "Noncontact tactile display based on radiation pressure of airborne ultrasound," *IEEE Transactions on Haptics*, vol. 3, no. 3, pp. 155–165, 2010.

[2] O. Georgiou, W. Frier, and O. Schneider, "User experience and mid-air haptics: Applications, methods, and challenges," *Ultrasound Mid-Air Haptics for Touchless Interfaces*, pp. 21–69, 2022.

[3] S. Inoue, Y. Makino, and H. Shinoda, "Active touch perception produced by airborne ultrasonic haptic hologram," in *2015 IEEE World Haptics Conference (WHC)*. IEEE, 2015, pp. 362–367.

[4] Y. Makino, Y. Furuyama, S. Inoue, and H. Shinoda, "Haptoclone (haptic-optical clone) for mutual tele-environment by real-time 3d image transfer with midair force feedback." in *CHI*, vol. 16. San Jose, CA, 2016, pp. 1980–1990.

[5] T. Romanus, S. Frish, M. Maksymenko, W. Frier, L. Corenthy, and O. Georgiou, "Mid-air haptic bio-holograms in mixed reality," in *2019 IEEE international symposium on mixed and augmented reality adjunct (ISMAR-Adjunct)*. IEEE, 2019, pp. 348–352.

[6] J. Martinez, A. Harwood, H. Limerick, R. Clark, and O. Georgiou, "Mid-air haptic algorithms for rendering 3d shapes," in *2019 IEEE International Symposium on Haptic, Audio and Visual Environments and Games (HAVE)*. IEEE, 2019, pp. 1–6.

[7] K. Harrington, D. R. Large, G. Burnett, and O. Georgiou, "Exploring the use of mid-air ultrasonic feedback to enhance automotive user interfaces," in *Proceedings of the 10th international conference on automotive user interfaces and interactive vehicular applications*, 2018, pp. 11–20.

[8] O. Georgiou, V. Biscione, A. Harwood, D. Griffiths, M. Giordano, B. Long, and T. Carter, "Haptic in-vehicle gesture controls," in *Proceedings of the 9th international conference on automotive user interfaces and interactive vehicular applications adjunct*, 2017, pp. 233–238.

[9] R. Montano, R. Morales, D. Pittera, W. Frier, O. Georgiou, and P. Cornelio, "Knuckles notifications: mid-air haptic feedback on the dorsal hand for hands-on-the-wheel driving," *Frontiers in Computer Science*, vol. 6, p. 1455201, 2024.

[10] G. M. Hung, N. W. John, C. Hancock, and T. Hoshi, "Using and validating airborne ultrasound as a tactile interface within medical training simulators," in *Biomedical Simulation: 6th International Symposium, ISBMS 2014, Strasbourg, France, October 16-17, 2014. Proceedings 6*. Springer, 2014, pp. 30–39.

[11] P. Balint and K. Althoefer, "Medical virtual reality palpation training using ultrasound based haptics and image processing," *Proc. Jt. Work. New Technol. Comput. Assist. Surg*, vol. 1, no. 2, 2018.

[12] S. Inoue, S. Suzuki, and H. Shinoda, "Multiunit phased array system for flexible workspace," in *Ultrasound Mid-Air Haptics for Touchless Interfaces*. Springer, 2022, pp. 241–260.

[13] B. W. Drinkwater, "The physical principles of arrays for mid-air haptic applications," in *Ultrasound Mid-Air Haptics for Touchless Interfaces*. Springer, 2022, pp. 313–334.

[14] R. Malkin, B. Kappus, B. Long, and A. Price, "On the non-linear behaviour of ultrasonic air-borne phased arrays," *Journal of Sound and Vibration*, vol. 552, p. 117644, 2023.

[15] K. Hasegawa and H. Shinoda, "Modulation methods for ultrasound midair haptics," in *Ultrasound Mid-Air Haptics for Touchless Interfaces*. Springer, 2022, pp. 225–240.

[16] W. Frier, A. Abdouni, D. Pittera, O. Georgiou, and R. Malkin, "Simulating airborne ultrasound vibrations in human skin for haptic applications," *IEEE Access*, vol. 10, pp. 15 443–15 456, 2022.

[17] G. Reardon, B. Dandu, Y. Shao, and Y. Visell, "Shear shock waves mediate haptic holography via focused ultrasound," *Science Advances*, vol. 9, no. 9, p. eadf2037, 2023.

[18] Z. Shen, M. K. Vasudevan, J. Kučera, M. Obrist, and D. Martinez Plasencia, "Multi-point stm: Effects of drawing speed and number of focal points on users' responses using ultrasonic mid-air haptics," in *Proceedings of the 2023 CHI Conference on Human Factors in Computing Systems*, 2023, pp. 1–11.

[19] R. Montano-Murillo, D. Pittera, W. Frier, O. Georgiou, M. Obrist, and P. Cornelio, "It sounds cool: Exploring sonification of mid-air haptic textures exploration on texture judgments, body perception, and motor behaviour," *IEEE Transactions on Haptics*, 2023.

[20] A. Raza, W. Hassan, T. Ogay, I. Hwang, and S. Jeon, "Perceptually correct haptic rendering in mid-air using ultrasound phased array," *IEEE Transactions on Industrial Electronics*, vol. 67, no. 1, pp. 736–745, 2019.

[21] L. Fan, A. Song, and H. Zhang, "Haptic interface device using cable tension based on ultrasonic phased array," *IEEE Access*, vol. 8, pp. 162 880–162 891, 2020.

[22] Z. Shen, Z. Morgan, M. K. Vasudevan, M. Obrist, and D. Martinez Plasencia, "Controlled-stm: A two-stage model to predict user's perceived intensity for multi-point spatiotemporal modulation in ultrasonic mid-air haptics," in *Proceedings of the CHI Conference on Human Factors in Computing Systems*, 2024, pp. 1–12.

[23] T. Morisaki, M. Fujiwara, Y. Makino, and H. Shinoda, "Non-vibratory pressure sensation produced by ultrasound focus moving laterally and repetitively with fine spatial step width," *IEEE Transactions on Haptics*, vol. 15, no. 2, pp. 441–450, 2021.

[24] T. Morisaki and Y. Ujitoko, "Towards intensifying perceived pressure in midair haptics: Comparing perceived pressure intensity and skin displacement between lm and am stimuli," in *International Conference on Human Haptic Sensing and Touch Enabled Computer Applications*. Springer, 2024, pp. 107–119.

[25] T. Morisaki, M. Fujiwara, Y. Makino, and H. Shinoda, "Comparing lateral modulation and amplitude modulation in phantom sensation," in *International Conference on Human Haptic Sensing and Touch Enabled Computer Applications*. Springer, 2020, pp. 122–130.

[26] L. Mulot, G. Gicquel, Q. Zanini, W. Frier, M. Marchal, C. Pacchierotti, and T. Howard, "Dolphin: A framework for the design and perceptual evaluation of ultrasound mid-air haptic stimuli," in *ACM Symposium on Applied Perception 2021*, 2021, pp. 1–10.

[27] T. Hoshi, "Introduction to ultrasonic mid-air haptic effects," in *Ultrasound Mid-Air Haptics for Touchless Interfaces*. Springer, 2022, pp. 1–20.